Journal of the Korean Physical Society, Vol. 45, No. 4, October 2004, pp. 897∼906

Variations in the Thermal Conductivity of Insulating Thin Films with Temperature and Pressure

Soon-Ho Choi*
3KMITech. Ltd., Korea Maritime University, Yeongdo-ku, Busan 606-791

Shigeo Maruyama
Department of Mechanical Engineering, The University of Tokyo, 7-3-1, Hongo, Bunkyo-ku, Tokyo 113-8654, Japan

(Received 21 May 2004)

The thermal conductivity of a solid thin film was investigated by using two nonequilibrium molecular dynamics (NEMD) methods and changing the calculation conditions. Solid argon was selected as a target material because it has a typical Lennard-Jones (L-J) potential; hence, there was no need to consider the contribution by free electrons to a thermal conductivity. The results were not influenced by the adopted NEMD method, and there were no appreciable effects due to changes in the calculation conditions. The thermal conductivities calculated by using the MD simulations were compared with the available experimental data obtained from the bulk state, and the system's temperature and internal stress were confirmed to affect the thermal conductivity. From our investigation, the internal stress is explicitly an important factor that influences the thermal conductivity of solids; a micro-scale system has a lower thermal conductivity than the bulk material does. The temperature dependence was also carefully investigated, and good qualitative agreement with existing experimental data was obtained.

PACS numbers: 44, 65
Keywords: Molecular dynamics, Phonon mean free path, Thermal conductivity, Thin film

I. INTRODUCTION

Owing to developments of nano- and micro-technologies, films with thicknesses up to a few angstrom can be deposited, and the applications of these thin films, such as semiconductors, micro-electro-mechanical systems (MEMS) and nano-electro-mechanical systems (NEMS), have been extended more and more in related industries [1, 2]. These newly growing technologies require the various devices to perform advanced functions with greatly reduced sizes. However, at the same time, one must thoroughly understand and analyze the new phenomena resulting from the extremely small sizes.

Recent research has shown that the thermal conductivity of an extremely thin film is significantly lower than that of the bulk state. However, existing theories based on macro-systems, that is a bulk state [3–9], have the application limits, which means that significant errors will occur in the thermal behaviors of micro-scale systems when those behaviors are calculated by using a macro-scale heat transfer theory without any consideration on the above-mentioned characteristic. This reduced thermal conductivity plays a crucial role in the design of the devices related with thin films. For example, heat generation from CPUs or electronic chips degrades their performance; hence, a possibility of failure in the intended functions exists if a reduced thermal conductivity is not considered appropriately in the designs of NEMS/MEMS devices.

In recent decades, many researchers have focused their attentions on the variations in the thermal conductivity with film thickness and have established a prediction method through experiments or molecular dynamics (MD) simulations. Recently, Schelling et al. reported that the inverse of a thermal conductivity (λ^{-1}) has a linear relation to the inverse of a system thickness (L^{-1}) [8]. Choi *et al.* showed that the thermal conductivity of a thin film could be quantitatively calculated from a phonon mean free path (MFP), which could be obtained from MD simulation results [9]. However, their simulations were performed in a freestanding state, which means that no internal stress exists in the system.

Lukes *et al.* also studied the thermal conductivity of solid argon by using an MD simulation [5]. However, their calculated results was largely scattered and, in the high temperature region, the thermal conductivity of a thin film was observed to be larger than that of the

*E-mail: choi_s_h@naver.com

bulk state. We conjecture that the over-estimated thermal conductivity of Lukes *et al.* might have resulted from the internal stress of the system, which means that their simulated system was in a highly compressed state due to an inappropriate intermolecular distance. On the other hand, Kaburaki and Yip reported that the thermal conductivity of solid argon, which was obtained from an equilibrium molecular dynamics (EMD) simulation, was lower than the experimental results [10]. Furthermore, they maintained a solid state of argon up to 100 K although solid argon begins to melt about 85 K in a freestanding state. Since EMD simulations are generally used to obtain the properties of a bulk material, comparing their simulations with our MD studies was methodologically unreasonable. The thermal conductivity of a simulated system should be larger than that of a real material because a real material inevitably contains some defects, dislocations, and grain boundaries. However, a simulated system is ordinarily prepared as a perfect crystal, which means that the simulated system has to have a larger thermal conductivity than a real material. Therefore, an appropriate MD method for determining the thermal conductivity of an extremely thin film is needed.

In this study, we performed simulations by using classical non-equilibrium molecular dynamics (NEMD) methods to investigate variations in the thermal conductivity with temperature and pressure. Also, we carefully investigated whether the simulation results were affected by changes in the boundary conditions or the calculation conditions. Solid argon was selected as a target material because it is a typical material represented by the Lennard-Jones (L-J) potential, which is the simplest intermolecular potential. Furthermore, there was no need to consider the contribution by free electrons to the thermal conductivity because argon is a non-conductor electrically, which means that energy transport was caused only by lattice vibrations, thus making the simulation easy to perform. The results from simulations were compared with experimental data when possible.

II. SIMULATION METHOD

1. Molecular Dynamics

First of all, an intermolecular potential function should be specified for the MD simulation because it is needed to calculate the intermolecular force. Once the intermolecular force is obtained, the time evolution of a system can be calculated from Newton's second law. As described in the Section I, we adopted the L-J potential for this study [9].

The new state of the N-molecule system in phase space, which is often referred as a hyper-space with 6N dimensions, was obtained by integrating the equation of motion. We used the Velocity-Verlet method with a truncation error of Δt^4 for the position evolution of the molecules, which was easily confirmed by using a Taylor expansion of the displacement [11–14]. In the Velocity-Verlet method, the simulation evaluates the intermolecular force, the velocity, and the new position of the molecule consecutively.

In addition to the Velocity-Verlet method, in order to integrate the equation of motion in the MD simulation, we can use other integration methods, such as the Leap-Frog method, the Verlet method, the Predictor-Corrector method, *etc.* However, there is no need to mention them here in detail because they can be easily found in other references [11–14].

2. Simulation System

The simulation system was arranged with the face centered cubic (fcc) structure shown in Fig. 1 because argon actually crystallizes in the fcc structure. The left diagram of Fig. 1 shows the cutting plane for the molecules' arrangement in the fcc<111> structure, and the planes are defined by the Miller indices [15]. We prepared two types of simulation systems to investigate whether differences of the boundary conditions might have an effect on the simulation results. Although the boundary conditions and the method of heat current creation were quite different, as will be explained below, the two systems had the same dimensions for direct comparison between them.

One system, hereafter referred to as SYS_1, had adiabatic walls at both ends, as shown in Fig. 2(a). These adiabatic walls, each of which was composed of 3 layers, were not movable, but were fixed throughout the simulation. Just on and below these adiabatic walls, the temperature control layers (TCLs) were placed, and each TCL consisted of 3 layers. The adiabatic walls were installed to isolate the system from the environment, and the TCLs were used to keep the two ends at the desired temperatures. The bottom TCLs were controlled to maintain the high temperature and the top the low temperature; therefore, the heat current flowed up (z

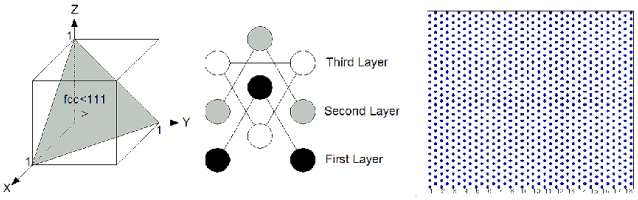

Fig. 1. The fcc<111> structure is defined by the Miller indices, and is cut as in the leftmost diagram. Three identical layers, as shown in the middle, are overlapped in the fcc<111> structure and the molecules' arrangement, when looking down from the top is viewed as shown in right diagram.

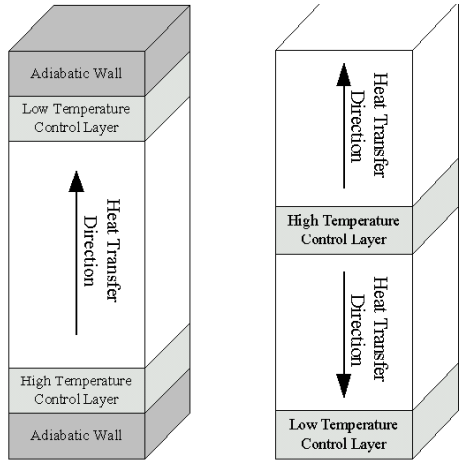

(a) 2-dimensional PBC (b) 3-dimensional PBC

Fig. 2. Two simulation systems used to investigate the effect resulting from the different boundary conditions: (a) the system with 2-dimensional PBC and the adiabatic walls at opposite ends (referred as SYS_1), and (b) the system with 3-dimensional PBC (referred as SYS_2). Temperature control for the TCLs is performed by velocity scaling for SYS_1 and velocity exchange for SYS_2.

direction). The $x-y$ plane perpendicular to the heat flow direction had a set of periodic boundary conditions (PBCs) to mimic an actual thin film. Actually, the SYS_1 is identical to the system used in our previous studies to evaluate the phonon mean free path (MFP) of a thin film and the thermal boundary resistance at the interfaces in superlattices [9, 16]. The other simulation system, hereafter referred to as SYS_2, is shown in Fig. 2 (b); this system has 3-dimensional PBCs. In SYS_2, the TCLs were placed at the bottom and in the middle, and each TCL was composed of 3 layers. The bottom TCLs were controlled to maintain the low temperature, and the middle TCLs the high temperature; therefore, heat current flowed from the middle to the two ends. The heat currents in both systems were created by using different methods, which was done to verify the methodology of our simulation methods. In addition to the different boundary conditions, we carefully investigated any effect that might be caused by changing the simulation conditions, which are described in detail in Section III.

The molecules were identically arranged with 18 each in the x and the y directions in both SYS_1 and SYS_2 with the exception of investigating the effect due to the heat transfer area, which is also described in Section III; hence, there are 324 molecules per layer. In SYS_1, the total number of layers was thirty, and the thermal conductivity was analyzed only for the middle 18 layers. That is, the fixed layers and the TCLs at both ends were excluded when evaluating the temperature gradient in the system. On the other hand, forty-two layers were stacked in the SYS_2; with the exclusion of the bottom and the middle TCLs, two sections of eighteen layers could be independently evaluated for a thermal conductivity, which means that one simulation run provided two evaluations for the thermal conductivity in SYS_2.

3. Temperature Control, Heat Flux and Thermal Conductivity

In the simulation system of SYS_1, the velocity scaling method was used to control the temperatures of the hot and the cold TCLs as follows:

$$v_{new}|_i = v_{old}|_i \sqrt{\frac{T_{des}}{T_i}}. \tag{1}$$

where v_{old} and v_{new} are the velocities before and after a velocity scaling, respectively. By making one TCL hot and the other TCL cold through Eq. (1), we could create a temperature gradient in the simulation system. In Eq. (1), T_{des} is the desired TCL temperature, and T_i is an individual molecule's instantaneous temperature in the TCLs as given by

$$T_i = \frac{m_i \cdot v_{old}|_i^2}{3k_B}, \tag{2}$$

where m_i is the mass of one molecule and k_B is the Boltzmann constant (1.381×10^{-23} J/K). The simulation parameters and the molecule's properties for this study are presented in Table 1. Besides the above velocity scaling method for the temperature gradient of the system, other methods are available, and a typical example is the phantom molecule method originating from the Langevin Equation [17–20]. However, since the phantom molecule method showed a large temperature jump between the imaginary phantom molecules and the system molecules [19,20], we selected the conventional, and simple velocity scaling method for temperature control of the TCLs.

In actual experiments, the thermal conductivity is generally obtained from measurements of the temperature gradient of a system and the heat flux through it. An NEMD simulation uses the same procedure as the real experiment. The heat flux is calculated from the energy input into a system to maintain the hot TCL at a high temperature or the energy removed from a system to hold the cold TCL at a low temperature during velocity scaling. Therefore, in SYS_1, as shown in Fig. 2(a), the heat currents are derived from the accumulated energy supplied to the hot TCL during a simulation, Eq. (3), or from the energy removed from the cold TCL, Eq. (4), because the velocity scaling method was used to maintain the temperature gradient in a system.

$$q_{in} = \frac{m}{2} \sum_{j=1}^{n_{TC}} \sum_{i=1}^{N_H} \left(v_{new}|_i^2 - v_{old}|_i^2 \right), \tag{3}$$

$$q_{out} = \frac{m}{2} \sum_{j=1}^{n_{TC}} \sum_{i=1}^{N_L} \left(v_{old}|_i^2 - v_{new}|_i^2 \right), \tag{4}$$

Table 1. The molecule's properties [13, 14] and the simulation parameters [9, 16].

m_{AR} (the mass of an argon molecule)	6.634×10^{-26} kg
σ_{AR} (the diameter of an argon molecule)	3.4 Å
ϵ_{AR} (the potential well depth of an argon molecule)	1.67×10^{-21} J
R_{CUT} (the cut-off length for an intermolecular interaction)	3.5 σ_{AR}
Δt (the time interval for an iteration)	1.0×10^{-15} s (1.0 fs)

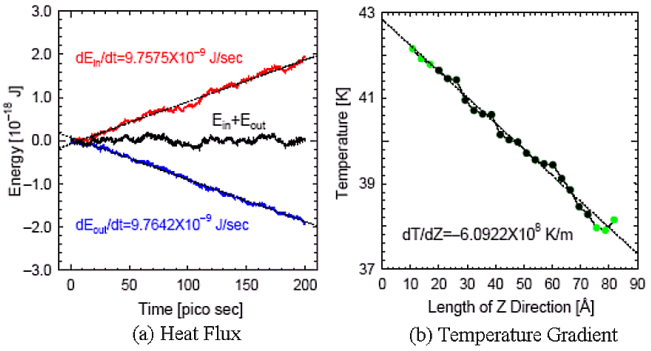

(a) Heat Flux (b) Temperature Gradient

Fig. 3. Heat flux and temperature gradient of SYS_1 with an average temperature of 40 K and with the velocity scaling. (a) The accumulated energies supplied to the hot TCLs and removed from the cold TCLs are nearly equal to each other if the system is in a fully NESS. (b) The temperatures of both TCLs (the gray circles) were excluded when evaluating the temperature gradient. These figures are cited from Ref. 9.

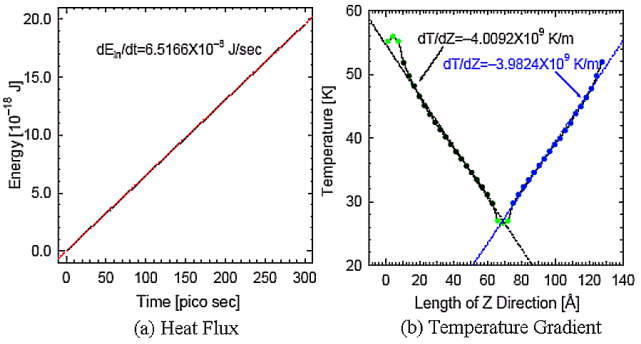

(a) Heat Flux (b) Temperature Gradient

Fig. 4. Heat flux and temperature gradient of SYS_2 with an average temperature of 40 K. For temperature control, the velocity exchange method was applied per every fifteen iteration. (a) The accumulated energies supplied to the hot TCLs. (b) The temperature profile developed in a system. The temperatures of both TCLs (the gray circles) were excluded when evaluating the temperature gradient. In the velocity exchange method, the heat flux flowing into the system is naturally equal to that flowing out of the system.

where N_H is the number of molecules in the hot TCL, N_L is that in the cold TCL, and n_{TC} is the total number of velocity scalings performed during a simulation.

In SYS_2, as shown in Fig. 2(b), we adopted a different method for obtaining a temperature gradient, which was proposed by F. Muller-Plathe and by Bedrov and Smith, and is called the velocity exchange method [21, 22]. Therefore, SYS_2 can be considered to be quite different from SYS_1 although it is prepared for the same purpose, that is, the calculation of the thermal conductivity. In the velocity exchange method, the fastest molecule in the cold TCL and the slowest molecule in the hot TCL are selected and their velocities are exchanged. Consequently, energy is added to the hot TCL and an identical energy is removed from the cold TCL by the velocity exchange. This method will not alter the total energy of the system; however, the velocity scaling will cause a fluctuation in the total energy whenever the scaling is performed. The heat currents obtained by using the velocity exchange are simply calculated from the exchanged kinetic energy:

$$q_{in} = q_{out} = \frac{1}{2}\left\{\frac{m}{2}\sum_{j=1}^{n_{TC}}(v_{fast}^2 - v_{slow}^2)\right\}, \qquad (5)$$

where n_{TC} is the total number of velocity exchanges performed during a simulation, v_{fast} is the fastest molecule's velocity in the cold TCL, and v_{slow} is the slowest molecule's velocity in the hot TCL. The first coefficient of one half on the right-hand side is necessary because the heat current flows in both directions, as shown in Fig. 2(b). The heat flux is calculated by dividing the above energies by the simulation time $(n \cdot \Delta t)$ and the heat transfer area (A).

If a fully nonequilibrium steady state (NESS) is developed in the system, the heat fluxes of Eqs. (3) and (4) will be equal to each other for the case of SYS_1. Figure 3 shows the heat fluxes and the temperature gradient from the MD simulation for SYS_1. The temperature profile was obtained by averaging the temperatures of all the molecules in a layer and is cited from our previous study [9]. The gray circles are the temperatures of the TCLs, and they were excluded when the temperature gradient was evaluated. From this figure, the heat fluxes from Eqs. (3) and (4) are indistinguishably equal, as with previous descriptions, (the maximum deviation of the two heat fluxes is under 0.1 % at most in all simulations) [9, 16]. The same results for SYS_2 are shown in Fig. 4, for which the heat current was created by using the velocity exchange method. However, it should be noted that the heat transfer rates shown in these figures have not been calculated per unit heat transfer area and per unit temperature difference. From a comparison of Figs. 3 and 4, it can be seen that the velocity exchange method can-

not control the TCLs' temperatures at an intended value while the velocity scaling method can. This feature results from the fact that we cannot predict the molecules' velocity distribution in the TCLs. Especially, the temperature gradient of SYS_2 is very large compared with that of SYS_1, which causes serious errors in the thermal conductivity evaluation. From the analyses of the simulation results, the velocity exchange method appears to have several unexpected defects that are described in Section III.

In this study, all simulations had 200,000 iterations per run; thus, one run corresponded to 200 ps (10^{-12} s) for the velocity scaling method and 300,000 iterations, that is 300 ps, for the velocity exchange method. The variations in the thermal conductivity due to changes in the initial setting conditions were investigated for average system temperatures of 10 K and 40 K. Thirteen runs were simulated for each case. The first run brought the system to the intended initial temperature, and the second run was for the relaxation, which meant that the system was left as it was without any manipulation. After the system had equilibrated at the desired temperature, a temperature difference was applied to both TCLs from the third simulation. However, this third run was excluded from the evaluation of the temperature gradient because it was certainly a transient period. Therefore, the thermal conductivity was evaluated over ten rest runs and averaged. Although we adopted the above-mentioned procedure for calculating the thermal conductivity, we were not sure that the two runs to attain system equilibrium were necessary, at least in the NEMD simulations. That is, there was no significant difference between the thermal conductivities evaluated from the simulations with and without the two runs to attain initial equilibrium.

For SYS_1, the thermal conductivity was calculated by using Eq. (4) based on the heat removed from the cold TCL because it corresponded to the real energy flowing out of the system. Because of the extremely thin film thicknesses, the heat fluxes approximately ranged from the order of 10^8 to 10^9 W·m^{-2}·K^{-1} in both systems. The evaluation of the thermal conductivity was done through Fourier's Law, though it was originally for the macro-system.

III. SIMULATION RESULTS

1. Effects from the Boundary Conditions and the Temperature Control Interval

As described previously, two systems with the different boundary conditions were used and, for a temperature gradient, different methods were applied to each system: that is, velocity scaling for SYS_1 and velocity exchange for SYS_2. The intermolecular lengths were selected so that the systems were in a freestanding state, the details

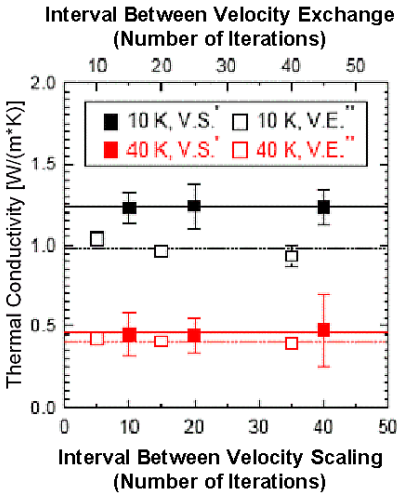

Fig. 5. Comparison of the thermal conductivities obtained from the different boundary conditions and temperature control methods. The effects due to changes in the temperature control intervals are shown together. V.S.* means the temperature control was carried out by using the velocity scaling method (the filled squares). V.E.** means the temperature control was carried out by using the velocity exchange method (the blank squares). The upper two lines are the thermal conductivities for a system average temperature of 10 K and the lower two lines are for 40 K. The error bar presents 3 σ_{STD} (the standard deviation).

of which are given in the following section. When the system maintained an average temperature of 10 K, the intermolecular length was 1.0969 σ_{AR}, and for the case of 40 K, it was 1.1115 σ_{AR} [9,16].

Figure 5 shows the calculated thermal conductivities of the two systems. The solid and the dotted lines present the results when velocity scaling was applied to SYS_1 and velocity exchange was applied to SYS_2, respectively; the upper two lines present the thermal conductivities when the system's average temperature was 10 K and the lower two lines are for 40 K. The filled squares are the thermal conductivities obtained from the simulations for SYS_1, and the blank squares are those for SYS_2. Since the error bar presents 3 σ_{STD} (the standard deviation), all data of each case are distributed within the range of the respective error bars. The results show that the interval of velocity scaling/exchange for the temperature control does not seriously affect the thermal conductivity. For the case of SYS_1, one temperature control per 10, 20, and 40 iterations was carried out through velocity scaling and one per 5, 15, and 35 iterations was carried out for the case of SYS_2 through velocity exchange. The maximum deviation between SYS_1 and SYS_2 is about 11 % for the average system temperature of 40 K and 26 % for 10 K. Actually, these deviations are acceptable for MD simulations because a very small number of molecules are simulated compared with a macro-system. Nevertheless, if we consider that ten values of the thermal conductivities were averaged, these deviations seem

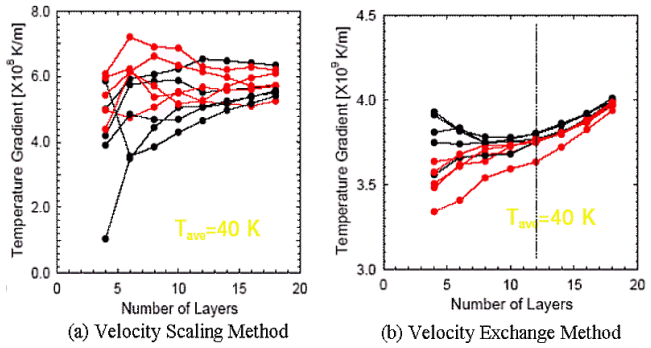

Fig. 6. Comparison of the slopes of the temperature gradients in SYS_1 and SYS_2. The average temperatures of the systems were both 40 K and each system were arranged with $18 \times 18 \times 18$ molecules. The slopes of the temperature gradients developed (a) for SYS_1 with the velocity scaling method and (b) for SYS_2 with the velocity exchange method. The axis of abscissas means the partial lengths were taken symmetrically from the center of a system to both end directions with a stepwise increment.

somewhat large and may eventually create large fluctuations in properties of interest.

To clarify the deviations due to the temperature control methods and the boundary conditions, we investigated carefully the temperature gradients in a system and found that the velocity exchange method caused the temperature gradient to be very high, as seen in Fig. 4. Consequently, this large temperature gradient created the nonlinearity, which can be seen as the type of S, and this nonlinearity increases much more as the interval of the velocity exchange is reduced. In the MD simulations of the thermal conductivity, this behavior is well known and inevitable. If the temperature gradient is decreased, fluctuations in temperatures become large. On the contrary, if the temperature gradient is increased to reduce the temperature fluctuations, an appreciable nonlinearity appears. Figure 6 shows the slopes of the temperature gradients measured over the partial length from the middle of a system, (a) for SYS_1 and (b) for SYS_2. The partial lengths were taken symmetrically from the middle to both end directions with a stepwise increment. As previously described, the thermal conductivity was averaged over ten runs; therefore, ten data are included in each graph. Apparently, a nonlinearity in the temperature gradient exists for the case of the velocity exchange method while the temperature gradients converge for the case of the velocity scaling method. From Fig. 6 (b), it is seen that the temperature gradients were roughly constant up to twelve layers, measured in both directions from the center of a system. Thus, when the velocity exchange method is used for the heat current, the temperature gradient should be evaluated over lengths that do not include the nonlinearity.

Figure 7 shows the thermal conductivities recalculated by using the newly obtained temperature gradients. In comparison with Fig. 5, the deviations due to the two

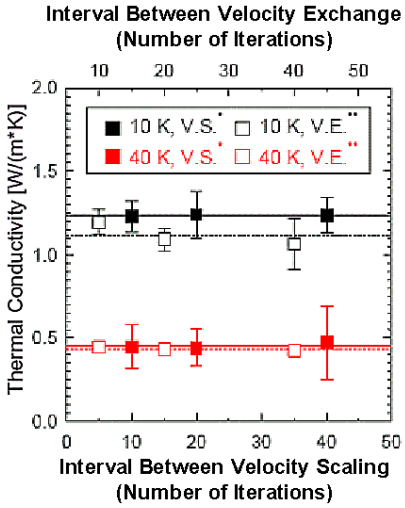

Fig. 7. Comparison of the thermal conductivities obtained from the different boundary conditions and the temperature control methods. The meanings of V.S.* and V.E.** are the same as in Fig. 5. The thermal conductivities (blank squares) obtained by using the velocity exchange method were recalculated by using the newly revaluated temperature gradient over the length of twelve layers in the middle of the system. From comparison with Fig. 5, the deviations were reduced.

methods to create the heat current and the different boundary conditions were apparently reduced. The maximum deviation between the average values was 4 % for the average system temperature of 40 K and 10 % for 10 K. Since the error bar is 3 σ_{STD} and all data of each case are within the respective error bars, it can be concluded that there are no effects due to the different boundary conditions and the different methods used to create a heat flow. However, the velocity exchange method has a defect; it leads to a very large temperature gradient, which may eventually cause a nonlinearity in the temperature gradient. Therefore, an accurate calculation of the thermal conductivity requires the additional task of evaluating the nonlinearity of the temperature gradient. Also, though the velocity exchange methods applied to SYS_2 can evaluate the thermal conductivity twice per one run, the running time is long compared with that for the velocity scaling method. That is, for the exchange of velocities, a procedure is necessary to sort the molecules' velocities, which imposes a burden on the CPU. For these reasons, we did not use the velocity exchange method further; rather we continued the following simulations only by using the velocity scaling methods applied to SYS_1. However, it should not be overlooked that the velocity exchange method has better energy conservation characteristics than any other method developed up to now.

2. Effects from the Heat Transfer Area and the Temperature Difference

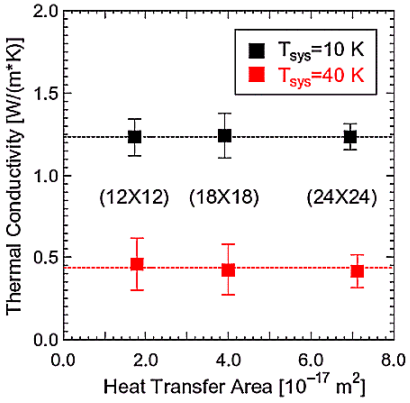

Fig. 8. Thermal conductivity versus heat transfer area for system temperature of 10 K and 40 K. The simulations were performed for SYS_1.

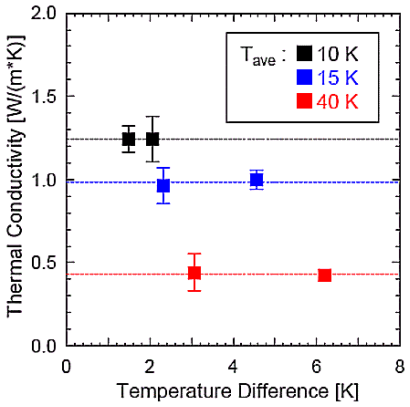

Fig. 9. Effect of the temperature difference, ΔT, on the thermal conductivity. The investigation was performed using SYS_1 with average temperatures of 10 K, 15 K, and 40 K. The top line is for T_{ave} = 10 K, the middle line is for 15 K, and the bottom line is for 40 K. The maxium ΔT, which was 4.55K and corresponded to about 30 % of T_{ave}, was applied for the case of T_{ave} = 15 K.

To investigate whether the initial value of the heat transfer area has an influence on the thermal conductivity, we made a series of the simulations for various heat transfer areas. Since the simulation system has a set of PBCs in the directions perpendicular to the heat flux, the heat transfer areas must not affect the thermal conductivity. However, surprisingly, at least within our survey of related references, this apparent fact has not been confirmed up to now, although it is considered to be just satisfied. Therefore, to verify the NEMD methodology used to evaluate the thermal conductivity, a need exists to confirm whether the heat transfer areas affect the thermal conductivity. For the sake of this, three heat transfer areas were simulated for SYS_1 as shown in Fig. 2(a). By arranging the molecules in 12 × 12, 18 × 18 and 24 × 24 arrays in the $x - y$ plane, we changed the heat transfer areas and simulated the systems for average temperatures of 10 K and 40 K. Figure 8 shows the variation of the thermal conductivity with the heat transfer area, and each datum point represents a value averaged over ten data, as explained in Section II-3. From the figure, the thermal conductivity can be confirmed to be independent of the heat transfer area. Actually, this feature must be just satisfied because the directions perpendicular to the heat flux were subjected to PBCs. If this were not so, our NEMD methodology would not be appropriate. Therefore, at least, the NEMD method used in this study is proper and mimics quite well the behavior of actual thin films.

In addition to effect of the heat transfer area, we carefully investigated whether any changes occurred in the thermal conductivity when various temperature differences were applied to both TCLs. For this, SYS_1 was initialized for three average temperatures (T_{ave} = 10 K, 15 K, and 40 K); then, various temperature differences ($\Delta T = 2 \sim 8$ K) were applied to both TCLs. However, the actual temperature differences, excluding the TCLs, ranged from 1.49 K to 6.18 K, as shown in Fig. 9. The maximum ΔT was applied for the average system temperature of 15 K and corresponded to about 30 % compared with T_{ave}. Since the error bars were also in the range of 3 σ_{STD}, it could be concluded that the temperature difference did not affect the thermal conductivity in the NEMD simulations. However, we cannot be sure that this conclusion will be justified even though ΔT exceeded 30 % of T_{ave}. We think that, compared with the average system temperature, a nonlinearity will appear in the temperature gradient if ΔT exceeds any threshold value.

3. Pressure and Temperature Effect on the Thermal Conductivity

The thermal conductivity, the most interesting thermal property of a material, is actually affected by the temperature and the pressure. In the cases of liquids and gases, experimental results as a function of the temperature or the pressure are plentiful. In solids, the effect on a thermal conductivity due to the temperature change is well known, but the effect due to the pressure has not been reported in detail, which may result from the fact that there is almost no high-pressure service condition for which the pressure dependence of the thermal conductivity plays a key role in heat transfer [23–25]. However, that is quite different in MD simulations because any change in the intermolecular distance results in a comparatively large deformation of the system, and consequently a great internal stress. This requires that the effect on the thermal conductivity due to a pressure change be investigated when performing MD simulations. If it is not, the calculated thermal conductivity could contain an additional effect due to the internal stress.

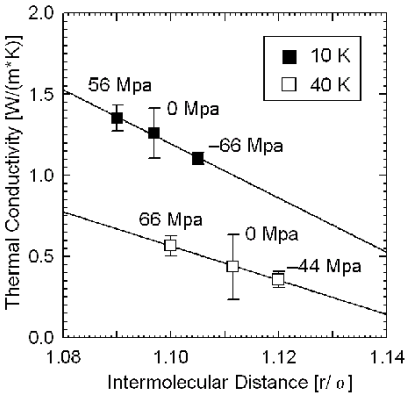

Fig. 10. Thermal conductivity of a thin film versus the intermolecular distance for various values of the internal stress. The pressure dependence seems to be significant at a lower system temperature.

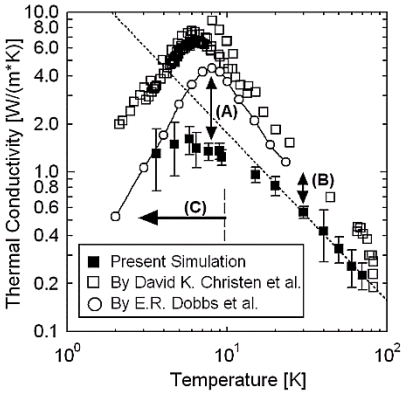

Fig. 11. Thermal conductivity versus system temperature. (A) and (B) shows the reduction of the thermal conductivity, which is a feature of thin films. (C) indicates the application limit of classical MD simulations. The data by Christen and Pollack are cited from Ref. 27 and those by Dobbs and Jones from Ref. 28.

It is easily supposed from one's physical intuition that the thermal conductivity of a nonconductor, such as argon, might be affected by an internal stress because transport of the lattice vibration energy will be facilitated as the intermolecular separation decreases. The intermolecular length for a freestanding state was selected so that a stress would not be built up in a system, as found in our previous studies [9,16] and the intermolecular length suggested in those studies showed better agreement with the experimental data [26,27] than the results given by Broughton and Gilmer [28].

Figure 10 shows the thermal conductivity obtained at various internal stresses for average system temperatures of 10 K and 40 K. The minus sign in Fig. 10 means that the system is under a tensile state and vice versa. These results are reasonable from the physical viewpoint since the energy transport due to molecular vibrations will be greater when the intermolecular distance gets shorter. Hence, it can be concluded that the thermal conductivity of solids increases as the system is compressed. Furthermore, the rate of increase of the thermal conductivity will be high for lower system temperatures.

Also, from knowledge of statistical thermodynamic or thermal physics, the thermal conductivity of solids is well known to be proportional to T^3 at extremely low temperatures and to $T^{-1.0}$ at relatively high temperatures [29–32]. These characteristics are deduced from the thermal conductivity of a gas based on the kinetic theory of gases as follows:

$$\lambda = \frac{1}{3} c_V \cdot v_P \cdot l_{MFP}, \tag{6}$$

where in the case of solids, c_V is the specific heat capacity of a phonon, l_{MFP} is the phonon mean free path (MFP), and v_P is the phonon velocity inherent in a material, which is often explained as an acoustic velocity. On the other hand, for gases or liquids, c_V is the specific heat capacity of the gas at constant volume, v_P is the average molecular velocity, and l_{MFP} is the MFP between intermolecular collisions [29–32]. Equation (6) suggests that the thermal conductivity is determined by the specific heat, c_V, and a phonon MFP, l_{MFP}.

From phonon theory, the phonon MFP becomes shorter as the system gets hotter because the phonon population is increased, which causes the collision frequency between the phonons to be high. Increased phonon collisions prevent phonons with high energies in the hot region from moving well to the cold region and vice versa, which means that the energy transport, and consequently the thermal conductivity, is low. Therefore, it is easily inferred that phonon scattering governs the thermal conductivity at high temperatures, so the thermal conductivity is proportional to T^{-1}. However, at extremely low temperatures, the thermal conductivity is not governed the phonon MFP any longer, but is dominated by c_V because its value approaches zero. In such a temperature region, the specific heat at constant volume is given as [29–32]

$$c_V(T) = \frac{12\pi^4}{5} R \left(\frac{T}{\theta_D} \right)^3 \tag{7}$$

where

$$\theta_D = \frac{h \cdot \nu_D}{k_B}. \tag{8}$$

In Eqs. (7) and (8), R is the universal gas constant, h is the Plank constant, θ_D is the Debye temperature, and ν_D is the Debye frequency of the material. From Eqs. (6), (7) and (8), the thermal conductivity can be inferred to be proportional to T^3 since, at extremely low temperatures, the population of excited phonons can be ignored.

To investigate the temperature effect on the thermal conductivity, we performed MD simulations for SYS_1 for various average temperatures in a freestanding state. The lowest average temperature of the system was set

as 3 K, and the highest was 70 K. Figure 11 shows the behavior of the thermal conductivity as the system temperature is changed. The dashed line is the fitting line for the results from 15 K to 70 K and shows that the thermal conductivity is proportional to $T^{-1.05}$, which excellently reproduces the theoretical value, $T^{-1.0}$. However, it should be noticed that the thermal conductivity for the simulated system is lower than the experimental values for the bulk solid [26,27]. This reduced thermal conductivity is a feature of a micro-scale system and actually results from the fact that the phonon MFP is governed by the thickness of a thin film.

The phonon scattering in a solid consists of four processes, which are collisions among (a) phonons, (b) phonons and any defect that exists in a system, (c) phonons and the boundary of a system, and (d) phonons and free electrons. However, the scattering resulting from (b) and (d) can be completely ignored since structural defects not exist in perfect crystals such as those used in this study, and there is no need to consider free electrons in argon. Therefore, if we consider only (a) and (c) [4,7,9], the phonon MFP is given by

$$\frac{1}{l_{MFP}} = \frac{1}{l_{BULK}} + \frac{1}{L_{SYS}}, \tag{9}$$

where l_{BULK} is the phonon MFP in the bulk state and L_{SYS} is the thickness of the system. When L_{SYS} becomes infinite, according to Eq. (9), l_{MFP} should be equal to l_{BULK} because the system is in the bulk state. Consequently, L_{SYS} does not contribute to the phonon MFP in the bulk state. On the other hand, L_{SYS} becomes dominant in the determination of l_{MFP} as the system becomes micro-sized. When the thickness of a thin film is shorter than the phonon MFP in a bulk state, l_{MFP} will depend on L_{SYS}, which means that the thermal conductivity will decrease as the film gets thinner. The marks of (A) and (B) in Fig. 11 correspond to this behavior since the simulated system has a length of about 50 Å. It should also be noted in Fig. 11 that the difference between the thermal conductivities for the bulk state and the thin film is smaller at high temperatures than it is at low temperatures. This results from the phonon population being related with the system temperature as described below.

The phonon is not real, but imaginary, and its population is not conserved, contrary to the molecules in a material. The phonon MFP becomes shorter as the system gets hotter because the phonon population increases, which causes the collision frequency of phonons to increase, thus, the phonon MFP will be short and the thermal conductivity will decrease. The decrease in the phonon MFP is more remarkable in a cold system than it is in a hot system in the case of a thin film. Initially, the phonon MFP in a hot system is short because there are more phonons than there are in a cold system. Therefore, the thickness of a thin film is not the main factor in determining the thermal conductivity for a hot state. In other words, the phonon MFP in a hot system is comparable to the thickness of the thin film. On the other hand, the phonon MFP may be larger than the thickness of the thin film when the system is in a cold state, which implies that the decrease in the thermal conductivity is more severe in thin films when the system temperature is relatively low. Therefore, it can be concluded that the thermal conductivity of thin films is small compared with that of the bulk state and that this behavior will be enhanced as the temperature of the system becomes lower.

IV. CONCLUSION

NEMD simulations were performed to grasp some features of the thermal conductivity of thin films, and by changing the calculation conditions and the boundary conditions, we confirmed that the simulation method used in this study was appropriate. Solid argon was selected as a target material to avoid considering the effect of free electrons although solid argon has limitations from the viewpoint of engineering applications. Nevertheless, the results of this study should provide engineers or researchers with fundamental information on the thermal conductivity of thin films as described below.

The temperature differences applied to both TCLs does not affect the thermal conductivity if they are below about 30 % of the average temperature of the system. In addition, the thermal conductivity is independent of the boundary conditions, the heat transfer areas, and the methods used to create the heat flow. However, the intermolecular distance is an important factor in the MD simulation because it can cause a system to be under a large internal stress. Therefore, if the intermolecular distance is not properly selected, the system will be under an excessive stress, which results in a thermal conductivity other than that of the freestanding bulk state. From the NEMD results of this study, it is apparent that the thermal conductivity increases as a system is compressed and vice versa. This pressure dependence of the thermal conductivity is more sensitive in a cold state. Furthermore, this study indicates that the temperature of a system affects the thermal conductivity. However, we do not greatly emphasize this feature since it is already well known. However, it is worthwhile noting that our NEMD simulation reproduces a real situation compared to other studies [5,10].

Another conclusion is the fact that the thermal conductivity of a thin film is surely lower than that of the bulk states even though the internal stress and the system temperature can affect it. The reduction of the thermal conductivity of a thin film is more sensitive at lower system temperatures. Moreover, it should be noted that the classical MD simulations have limits. From Fig. 11, the thermal conductivity is maximum about at 10 K in both the experimental data and the simulation results. All solids have peak thermal conductivities at extremely

low temperatures, which is inherent to the material. The thermal conductivity of a solid rapidly decreases if the system temperature falls into a region in which the quantum effect is dominant. The rate of decrease is proportional to T^3, as described in Section III, because the classical laws are no more applicable due to the presence of quantum effects. This study is based on the classical MD method, so it cannot be extended to temperatures lower than 10 K, in principle. As shown in Fig. 11, the arrow (C) indicates the limit of this study. However, a need exists to make a thorough study as to why the classical MD results for the thermal conductivity show a maximum value just as real experiments because no quantum phenomena were involved in the simulations. Actually, from the large fluctuations of the thermal conductivities below 10 K seen in Fig. 11, we cannot be conclusively sure whether the classical MD simulations reproduce the behavior of the thermal conductivity even at extremely low temperatures where the quantum effect appears. Because the lowest average temperature of the system was selected as 3 K in this study, a temperature difference of at most 1 K, for the heat flux, can be applied to the system. This low temperature difference inevitably increases the fluctuations in the temperature gradient; consequently, the calculated thermal conductivities might be seen as values just for region (C) of Fig. 11. Therefore, for confirmation whether the classical MD simulations reproduce the actual behavior of the thermal conductivity of solids, other materials with maximum thermal conductivities at relatively high temperatures should be simulated. For that purpose, the simulations with other solid materials are being carried out at present, and we expect to be able to report the results soon.

REFERENCES

[1] T. Shinjo and T. Takada, *Metallic Superlattices-Artificially Structured Materials* (Elsevier, Amsterdam, 1987).

[2] S. E. Lyshevski, *Nano- and Microelectromechanical Systems* (CRC Press, New York, 2001).

[3] M. I. Flik and C. L. Tien, ASME J. Heat Transfer **112**, 872 (1990).

[4] M. I. Flik, B. I. Choi and K. E. Goodson, ASME J. Heat Transfer **114**, 666 (1992).

[5] J. R. Lukes, D. Y. Li, X. G. Liang and C. L. Tien, ASME J. of Heat Transfer **122**, 536 (2000).

[6] S. H. Choi and S. Maruyama, *Proceeding. of the 39th National Heat Transfer Symp.* (Sapporo, Japan, 2002).

[7] S. H. Choi, *Ph.D. Dissertation*, Tokyo University, Tokyo, 2003.

[8] P. K. Schelling, S. R. Phillpot and P. Keblinski, Phys. Rev. B **65**, 144306 (1997).

[9] S. H. Choi, S. Maruyama, K. K. Kim and J. H. Lee, J. Korean Phys. Soc. **43**, 747 (2003).

[10] H. Kaburaki and S. Yip, Proc. Mat. Res. Soc. **538**, 503 (1999).

[11] R. J. Sadus, *Molecular Simulation of Fluids-Theory, Algorithms and Object-Orientation* (Elsevier, Amsterdam, 1999).

[12] D. Frenkel and B. Smit, *Understanding Molecular Dynamics-from Algorithms to Applications* (Academic Press, New York, 1996).

[13] M. P. Allen and D. J. Tildesley, *Computer Simulation of Liquids* (Oxford Univ. Press, London, 1993).

[14] M. Haile, *Molecular Dynamics Simulation-Elementary Methods* (Wiley, New York, 1997).

[15] C. Kittel, *Introduction to Solid State Physics* (Wiley, New York, 1996).

[16] S. H. Choi, S. Maruyama, K. K. Kim and J. H. Lee, J. Korean Phys. Soc. **44**, 317 (2004).

[17] J. Blömer and A. E. Beylich, *Proceeding of the 20th Int. Symp. of Rare. Gas Dynamics*, (Beijing, August, 1997) p. 392.

[18] J. Blömer and A. E. Beylich, Surface Sci. **423**, 127 (1999).

[19] S. Maruyama and Soon-Ho Choi, Therm. Sci. Eng. **9**, 17 (2001).

[20] S. Maruyama, Micro. Thermophys. Eng. **7**, 41 (2003).

[21] F. Muller-Plathe, J. Chem. Phys. **106**, 6082 (1997).

[22] D. Bedrov and G. D. Smith, J. Chem. Phys. **113**, 8080 (2000).

[23] R. B. Bird, W. E. Stewart and E. N. Lightfoot, *Transport Phenomena* (Wiley, New York, 2002).

[24] Lindon C. Thomas, *Heat Transfer-Professional Version* (Prentice Hall, New York, 1993).

[25] G. F. Hewitt, G. L. Shires and Y. V. Polezhaev, *International Encyclopedia of Heat & Mass Transfer* (CRC Press, New York, 1997).

[26] E. R. Dobbs and G. O. Jones, Rep. Pro. Phys. **20**, 516 (1957).

[27] D. K. Christen and G. L. Pollack, Phys. Rev. B **12**, 3380 (1975).

[28] J. Q. Broughton and G. H. Gilmer, J. Chem. Phys. **70**, 5095 (1983).

[29] C. Kittel and H. Kroemer, *Thermal Physics* (Freeman, San Francisco, 1980).

[30] F. Reif, *Fundamentals of Statistical and Thermal Physics* (McGraw-Hill, London, 1985).

[31] J. E. Lay, *Statistical Mechanics and Thermodynamics of Matter-An Introductory Survey* (Harper & Row, New York, 1990).

[32] J. S. Blakemore, *Solid State Physics* (Cambridge University Press, London, 1985).